

1 **Supplementary information**

2 **Materials and Methods**

3 **Ethics statement**

4 All mouse and macaque studies were conducted under protocols approved by the  
5 Institutional Animal Care and Use Committee of the University of Science and Technology of  
6 China (Approved No. USTCACUC1801038). All procedures performed on Syrian hamster  
7 were in accordance with regulations and established guidelines, and were reviewed and  
8 approved by the Animal Ethics Committee of the Wuhan Institute of Virology, Chinese  
9 Academy of Sciences (Approved No. WIVA45202201). The animals received care in  
10 compliance with the guidelines outlined in the Guide for the Care and Use of Laboratory  
11 Animals.

12

13 **Cells and viruses**

14 HEK293T cells, Vero cells, and Vero E6 cells were cultured in Dulbecco's modified Eagle's  
15 medium (DMEM, Gibco) supplemented with 10% fetal bovine serum (FBS, ExCell Bio) and  
16 1% penicillin-streptomycin (Gibco) at 37°C under a 5% CO<sub>2</sub> atmosphere. The SARS-CoV-2  
17 WIV04 strain was initially isolated from an early severe COVID-19 patient in 2019 (GISAID  
18 accession no. EPI\_ISL\_402124); Delta variant (B.1.617.2; GWHBEBW01000000) by Prof.  
19 Hongping Wei; Beta variant (NPRC2.062100001) and Omicron variant (CCPM-B-V-049-  
20 2112-18) was kindly obtained from National Pathogen Resource Center. All processes in this  
21 study involving authentic SARS-CoV-2 were performed in the biosafety level 3 (BSL-3)  
22 facility in Wuhan Institute of Virology, Chinese Academy of Sciences.

23

## 24 **mRNA design and synthesis**

25 Spike (S) protein encoded by S<sub>WT</sub>-2P vaccine was designed from original ancestral SARS-  
26 CoV-2 WA1 (GenBank MN908947.3), and S<sub>Omicron</sub>-6P was based on a background of S  
27 sequences from SARS-CoV-2 variant Omicron (B.1.1.529) (GISAID: GR/484A). Both  
28 mRNAs were synthesized in vitro using an optimized T7 RNA polymerase-mediated  
29 transcription reaction with complete replacement of uridine by N1-methyl-pseudouridine. The  
30 reaction included a DNA template containing the open reading frame flanked by 5' untranslated  
31 region (UTR) and 3' UTR sequences and was terminated by an encoded poly A tail. The  
32 template for the S<sub>WT</sub>-2P mRNA is a DNA fragment encoding SARS-CoV-2 S with K986P and  
33 V987P substitutions, while that for the S<sub>Omicron</sub>-6P mRNA encoding Omicron variant S with  
34 F817P, A892P, A899P, A942P, K986P, and V987P substitutions.

35 The mRNA was purified by oligo-dT affinity purification, buffer exchanged by tangential  
36 flow filtration into sodium acetate, and sterile filtered. RNA integrity was assessed by  
37 microfluidic capillary electrophoresis (Fragment Analyzer systems 5200, Agilent), and the  
38 concentration, pH, residual DNA, proteins, and dsRNA impurities of the solution were  
39 determined. The mRNA 5' capping efficiency and 3'-polyadenosine (poly A) tail of mRNAs  
40 was studied using liquid chromatography coupled to mass spectrometry (LC-MS).

41

## 42 **mRNA encapsulation**

43 mRNAs were encapsulated in lipid nanoparticles (LNPs) using a modified procedure of a  
44 method previously as previously described.<sup>1</sup> Briefly, an ethanolic lipid mixture of ionizable

45 cationic lipid, phosphatidylcholine, cholesterol, and polyethylene glycol-lipid was rapidly  
46 mixed with an aqueous solution containing mRNA. The drug product underwent analytical  
47 characterization, which included the determination of particle size and polydispersity,  
48 encapsulation, pH, endotoxin, and bioburden, and the material was deemed acceptable for in  
49 vivo study.

50

#### 51 **mRNA transfection**

52 HEK293T were seeded in 24-well plates at  $1.5 \times 10^4$  cells/well, and transfected with  
53 S<sub>Omicron</sub>-6P mRNA using Lipofectamine<sup>®</sup> Messenger MAX<sup>™</sup> Reagent (Invitrogen) 12 h later  
54 according to the manufacturer's protocol.

55

#### 56 **Vaccine antigen detection by immunofluorescence**

57 Transfected HEK293T cells were fixed in 4% paraformaldehyde (PFA) and permeabilized  
58 with PBS/0.1% Triton X-100. After blocked with 1% BSA for 0.5 h at room temperature, the  
59 cells were incubated with SARS-CoV-2 Omicron S protein antibody (Sino Biological, 40592-  
60 R0004). The cells were stained with a fluorescent anti-rabbit IgG antibody (Abcam, ab6717),  
61 and DAPI (Sigma-Aldrich, 28718-90-3). Images were acquired with a laser scanning confocal  
62 microscope (Nikon A1).

63

#### 64 **Mouse immunizations**

65 All the control vaccines were generated to target the WT SARS-CoV-2 strain. CoronaVac,  
66 a 500  $\mu$ L dose, contains 3  $\mu$ g of SARS-CoV-2 virion with 225  $\mu$ g of aluminum hydroxide for

67 an adult. ZF2001, a 500  $\mu\text{L}$  dose, contains 25  $\mu\text{g}$  RBD-dimer protein with 250  $\mu\text{g}$  of aluminum  
68 hydroxide for an adult. The dosages of CoronaVac and ZF2001 applied in mice ranged from  
69 1/50 to 1/5 corresponding human dose, that is 0.3 (50  $\mu\text{L}$ ) and 0.6 (100  $\mu\text{L}$ )  $\mu\text{g}$  for CoronaVac  
70 group, 0.5 (10  $\mu\text{L}$ ), 2.5 (50  $\mu\text{L}$ ), and 5 (100  $\mu\text{L}$ )  $\mu\text{g}$  for ZF2001 group. mRNA vaccines,  
71 including S<sub>WT</sub>-2P (100  $\mu\text{g}$  mRNA of S for an adult), applied in mice ranged from 1/100 to 1/10  
72 corresponding human dose, that is 1, 5, and 10  $\mu\text{g}$  for S<sub>WT</sub>-2P and S<sub>Omicron</sub>-6P groups.

73 Female BALB/c mice (8–12 weeks old) were randomly allocated to groups. Mice were  
74 intramuscularly (i.m.) immunized with the same dose at 21-day intervals for mRNA vaccines  
75 or 28-day intervals for inactivated vaccine or protein subunit vaccine. Sera were collected on  
76 day 0, 21, 28, 35, and 42 after the first immunization to detect SARS-CoV-2 neutralizing  
77 antibodies (nAbs) titers as described below.

78

### 79 **Hamster immunization and challenge experiments**

80 Four groups of female Syrian hamsters (6–7 weeks old) were vaccinated on day 0 and day  
81 21 with 1, 10, 25, or 50  $\mu\text{g}$  of S<sub>Omicron</sub>-6P for prime-boost vaccine regimens by intramuscular  
82 injection to each hind thigh, while control hamsters were administered with PBS. On day 30,  
83 all animals were challenged intranasally with  $1 \times 10^4$  PFU of authentic SARS-CoV-2 Omicron  
84 virus after anesthetization with isoflurane.

85

### 86 **Macaque immunizations**

87 Male macaques (3–5 years old) were randomly assigned to receive S<sub>Omicron</sub>-6P (20 or 100  
88  $\mu\text{g}$ ) on day 0 and 21. The vaccine was i.m. administered in the quadriceps muscle. Sera were

89 collected on day 0, 21, 28, and 35 after the first immunization.

90

### 91 **Plaque reduction neutralization assay**

92 The plaque reduction neutralization assay was carried out as described previously.<sup>2</sup> Briefly,  
93 sera were inactivated at 56°C for 30 min before use. The sera were 3-fold serially diluted  
94 (started at 1:150) with DMEM containing 2.5% FBS, and mixed with an equal volume of  
95 authentic SARS-CoV-2 viruses incubated at 37 °C for 1 h. The mixture was added to Vero E6  
96 monolayer cells in 24-well plates. After another 1 h incubation at 37 °C, the mixture was  
97 replaced with DMEM containing 2.5% FBS and 0.9% carboxymethyl cellulose. The plates were  
98 incubated in a 5% CO<sub>2</sub>-air incubator at 37°C for 4 days, then fixed with 8% paraformaldehyde  
99 and stained with 0.5% crystal violet. The neutralization percentage was calculated as: (1- plaque  
100 number / plaque number without serum) × 100%. The IC<sub>50</sub> was analyzed using GraphPad  
101 Prism software with the “inhibitor vs normalized response (Variable slope)” model.

102

### 103 **Viral RNA load by RT-qPCR**

104 Quantitative reverse transcription PCR (qRT-PCR) was applied to measure the viral RNA  
105 loads in infected tissues.<sup>3</sup> Briefly, viral RNA were extracted from nasal turbinate and lung tissue  
106 homogenates with the QIAamp Viral RNA Mini Kit (Qiagen), and quantified using HiScript®  
107 II One Step qRT-PCR SYBR® Green Kit (Vazyme Biotech) with the primers ORF 1a/b-F (5'-  
108 CCCTGTGGGTTTTACTTAA-3') and ORF 1a/b-R (5'-ACGATTGTGCATCAGCTGA-3').  
109 ORF1a/b spans 16 non-structural proteins (NSPs) that are related to the replication-  
110 transcription complex of SAR-CoV-2. The primer-probe sets were based on sequence from

111 China CDC and have been demonstrated as the most sensitive one for molecular diagnosis of  
112 SARS-CoV-2 using qRT-PCR. The amplification procedures were set up as the following:  
113 50 °C for 3 min, 95 °C for 30 s followed by 40 cycles consisting of 95 °C for 10 s, 60 °C for  
114 30 s, and a default melting curve step in CFX96 System (Bio-Rad). The standard curve was  
115 generated using serial dilutions of SARS-CoV-2 ORF1ab gene control plasmid. The detection  
116 limit was determined by the standard curve and was about 120 copies per gram biopsy samples.  
117 The viral loads were calculated as the genome copies of SARS-CoV-2 in one gram tissues.

118

#### 119 **Infectious virus titer by plaque assay**

120 Infectious virus titer was determined with plaque assay as previously described with slight  
121 modification.<sup>4</sup> Briefly, animal tissue homogenates were serially 10-fold diluted with DMEM  
122 containing 2.5% FBS, and inoculated to Vero E6 seeded overnight at  $1.5 \times 10^5$  /well in 24-well  
123 plates; after incubated at 37°C for 1 h, the inoculate was replaced with DMEM containing 2.5%  
124 FBS and 0.9% carboxymethyl-cellulose. The plates were fixed with 8% paraformaldehyde and  
125 stained with 0.5% crystal violet 4 days later. Virus titer was calculated with the dilution gradient  
126 with 10~100 plaques.

127

#### 128 **Statistical analysis**

129 All data were analyzed with GraphPad Prism 8.0 software. Unless specified, data are  
130 presented as mean  $\pm$  SEM in all experiments. Analysis of variance (ANOVA) or t-test was used  
131 to determine statistical significance among different groups (\* $P < 0.05$ ; \*\*  $P < 0.01$ ; \*\*\*  $P <$   
132  $0.001$ ; \*\*\*\* $P < 0.0001$ ).

133

134 **REFERENCES**

- 135 1. Maier, M. A. et al. *Mol. Ther.* **21**, 1570-1578 (2013).  
136 2. Wang, Z. J. et al. *Emerg. Microbes. Infect.* **9**, 2606-2618 (2020).  
137 3. Feng, L. et al. *Nat. Commun.* **11**, 4207 (2020).  
138 4. Zhang, Q. et al. *Emerg. Microbes. Infect.* **9**, 2013-2019 (2020).

139

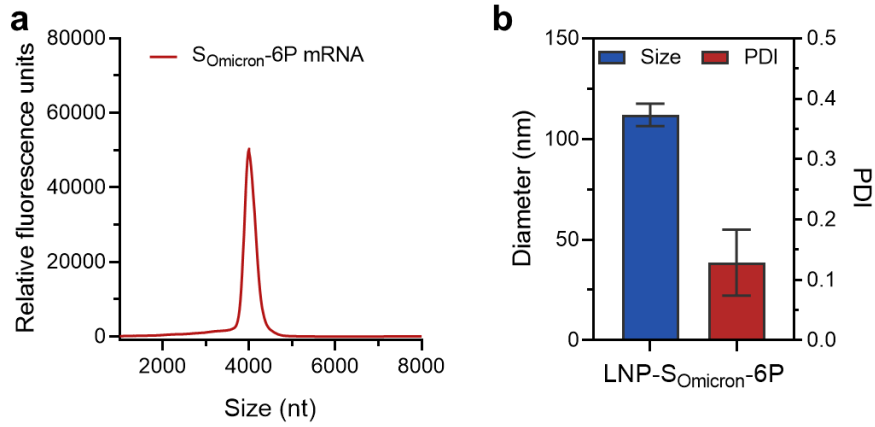
**Table S1. Amino acid sequence alignment of the full S protein of S<sub>omicron</sub>-6P.**

```

MFVFLVLLPLVSSQCVNLTTRTQLPPAYTNSFTRGVYYPDKVFRSSVLHSTQDLFLP
FFSNVTWFHVISGTNGTKRFDNPVLPFNDGVYFASIEKSNIIRGWIFGTTLDSKTQSL
LIVNNATNVVIKVCEFQFCNDPFLDHKNNKSWMESEFRVYSSANNCTFEYVSQPFL
MDLEGKQGNFKNLREFVFKNIDGYFKIYSKHTPIIVRDLPQGFSALEPLVDLPIGINI
TRFQTLALHRSYLTPGDSSSGWTAGAAAYYVGYLQPRTFLLKYNENGTITDAVDC
ALDPLSETKCTLKSFTVEKGIYQTSNFRVQPTEIVRFPNITNLCPFDEVFNATRFAS
VYAWNRKRISNCVADYSVLYNLAPFFTFKCYGVSPTKLNDLCFTNVYADSFVIRGD
EVRQIAPGQTGNIADYNYKLPDDFTGCVIAWNSNKLDSKVSIGNYNYLYRFRKSN
LKPFERDISTEIQAGNKPCNGVAGFNCYFPLRSYSFRPTYGVGHQPYRVVLSFEL
LHAPATVCGPKKSTNLVKNKCVNFNFNGLKGTGVLTESNKKFLPFQQFGRDIADTT
DAVRDPQTLEILDITPCSFGGVSVITPGTNTSNQVAVLYQGVNCTEVPVAIHADQLTP
TWRVYSTGSNVFQTRAGCLIGA EYVNNSYECDIPIGAGICASYQTQTKSHRRARSV
ASQSIIAYTMSLGAENSVAYSNNSIAIPTNFTISVTTEILPVSMTKTSVDCTMYICGDS
TECSNLLLQYGSFCTQLKRALTGIAVEQDKNTQEVFAQVKQIYKTPPIKYFGGFNFS
QILPDPSKPSKRSPIEDLLFNKVTLADAGFIKQYGDCLGDIAARDLICAQKFKGLTV
LPPLLTDEMIAQYTSALLAGTITSGWTFGAGPALQIPFPMQMAYRFNGIGVTQNVLY
ENQKLIANQFN SAIGKIQDSLSTPSALGKLQDVVNHNAQALNTLVKQLSSKFGAIS
SVLNDIFSR LDPPEAEVQIDRLITGRLQSLQTYVTQQLIRAAEIRASANLAATKMSEC
VLGQSKRVDFCGKGYHLMSFPQSAPHGVVFLHVTVVPAQEKNFTTAPAICHGKA
HFPREGV FVSNGTHWFVTQRNFYEPQIITDNTFVSGNCDVVIGIVNNTVYDPLQPE
LDSFKEELDKYFKNHTSPDVDLGDISGINASVVNIQKEIDRLNEVAKNLNESLIDLQ
ELGKYEQYIKWPWYIWLGFIAGLIAIVMVTIMLCCMTSCCCLKGCCSCGSCCKFD
EDDSEPV LKGVKLHYT

```





142

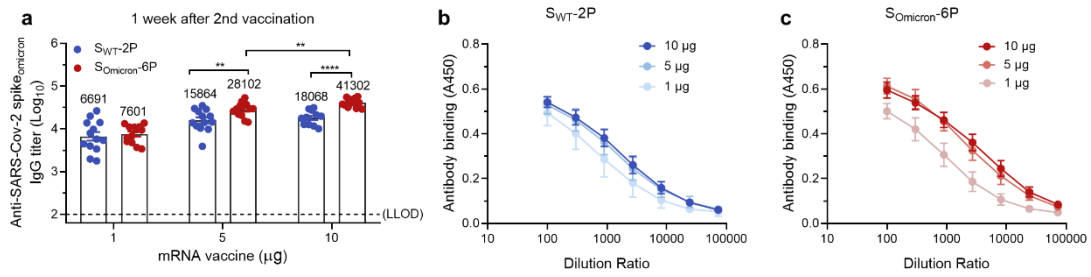
143 **Fig. S1. SARS-CoV-2 Omicron mRNA vaccine characterization.**

144 **a** Liquid capillary electropherograms of in vitro-transcribed S<sub>Omicron-6P</sub> mRNA.

145 **b** Sizes and polydispersity index (PDI) values of lipid nanoparticles (LNP) encapsulated with

146 S<sub>Omicron-6P</sub> mRNA. Data are shown as mean ± SD.

147

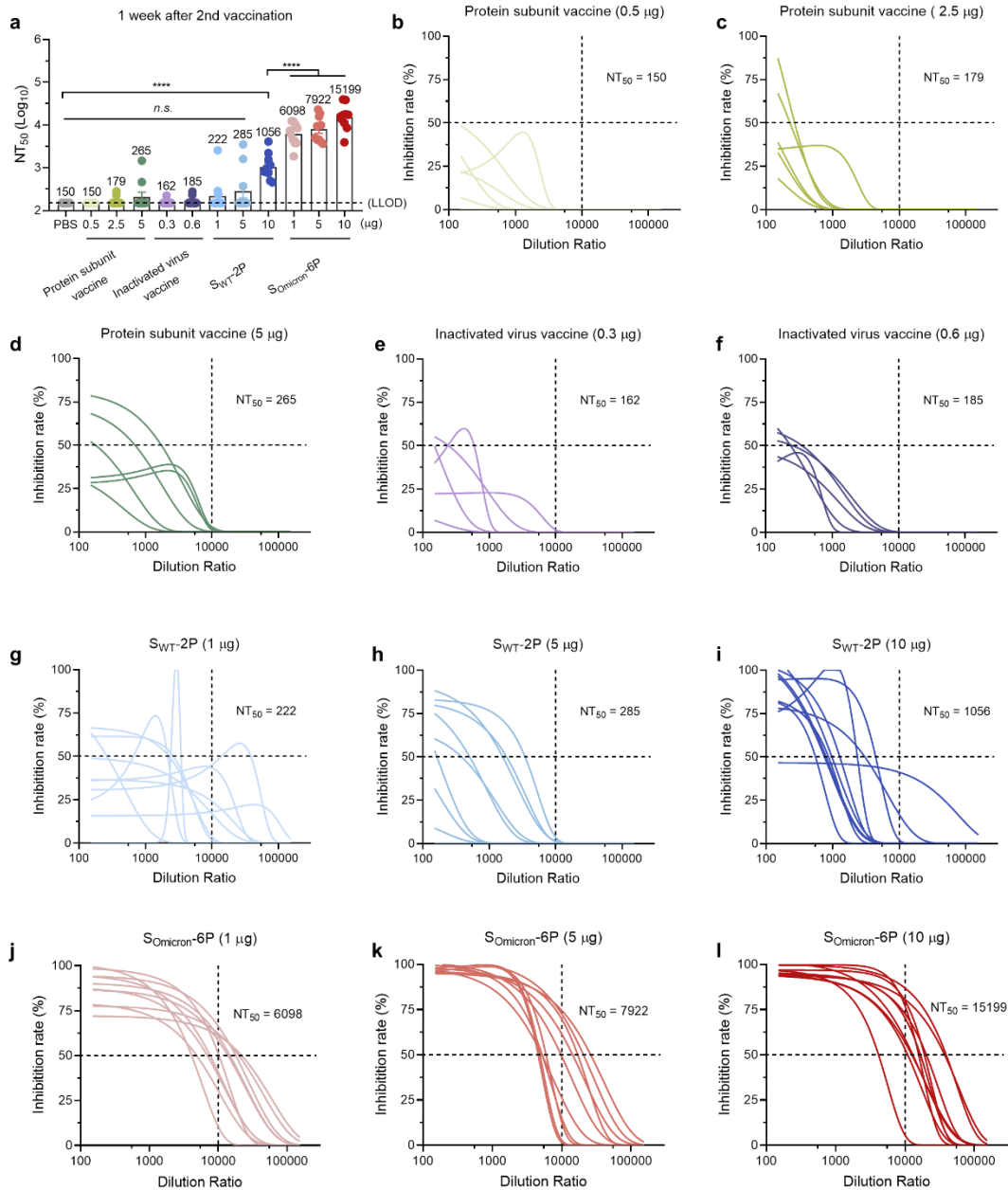


148

149 **Fig. S2. S<sub>Omicron-6P</sub> or S<sub>WT-2P</sub> elicits binding antibodies in mice.**

150 **a** The Omicron SARS-CoV-2 variant specific IgG antibody titers were determined by ELISA  
151 (lower limit of detection (LLOD) = 100) (*n* = 13).

152 **b, c** ELISA binding curves of S<sub>WT-2P</sub> (a) or S<sub>Omicron-6P</sub> (b) induced binding antibodies in mouse  
153 sera (*n* = 13).  
154



155

156 **Fig. S3. S<sub>Omicron</sub>-6P induces high levels of nAbs against pseudovirus of Omicron variant in**  
 157 **mice.**

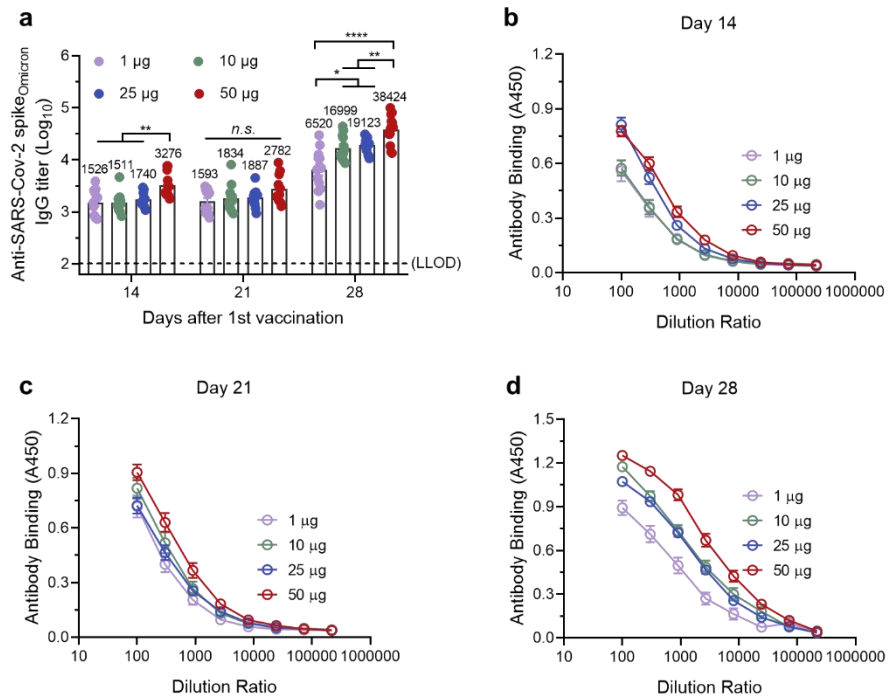
158 **a** Neutralization titers (NT<sub>50</sub>) were determined by recombinant vesicular stomatitis virus  
 159 (VSV)-based pseudovirus (Omicron variant) neutralization assay (LLOD = 150) ( $n = 6\sim 10$ ).

160 **b-d** Neutralization curves of 0.5 (b), 2.5 (c), and 5 (d)  $\mu\text{g}$  protein subunit vaccine (25  $\mu\text{g}/\text{vial}$   
 161 for an adult) induced nAbs against pseudotyped and replication-deficient SARS-CoV-2  
 162 Omicron ( $n = 6$ ).

163 **e, f** Neutralization curves of 0.3 (e), and 0.6 (f)  $\mu\text{g}$  inactivated virus vaccine (3  $\mu\text{g}/\text{vial}$  for an  
 164 adult) induced antibodies against pseudotyped and replication-deficient SARS-CoV-2  
 165 Omicron ( $n = 6$ ).

166 **g-i** Neutralization curves of 1 (g), 5 (h), and 10 (i)  $\mu\text{g}$  S<sub>WT</sub>-2P induced antibodies against

167 pseudotyped and replication-deficient SARS-CoV-2 Omicron ( $n = 10$ )  
168 **j-l** Neutralization curves of 1 (j), 5 (k), and 10 (l)  $\mu\text{g}$   $S_{\text{Omicron-6P}}$  induced antibodies against  
169 pseudotyped and replication-deficient SARS-CoV-2 Omicron ( $n = 10$ ).  
170



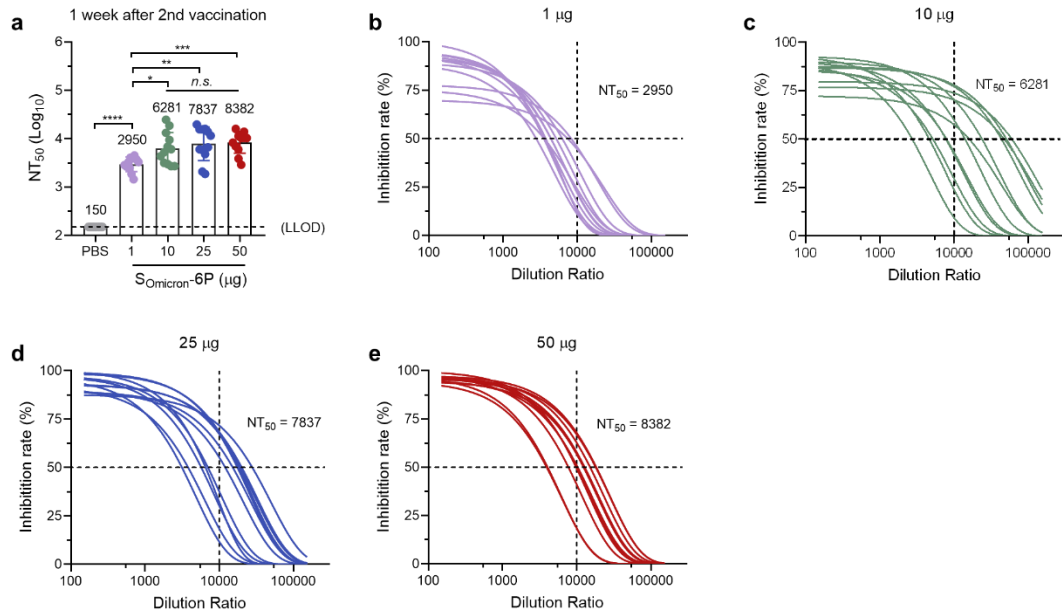
172

173 **Fig. S4. S<sub>Omicron</sub>-6P elicits binding antibodies in hamsters.**

174 **a** The Omicron SARS-CoV-2 variant specific IgG antibody titers were determined by ELISA  
 175 (LLOD = 100) (*n* = 12).

176 **b-d** ELISA binding curves of S<sub>Omicron</sub>-6P induced antibodies in hamster sera on day 14 (b), day  
 177 21 (c), and day 28 (d) (*n* = 12).

178



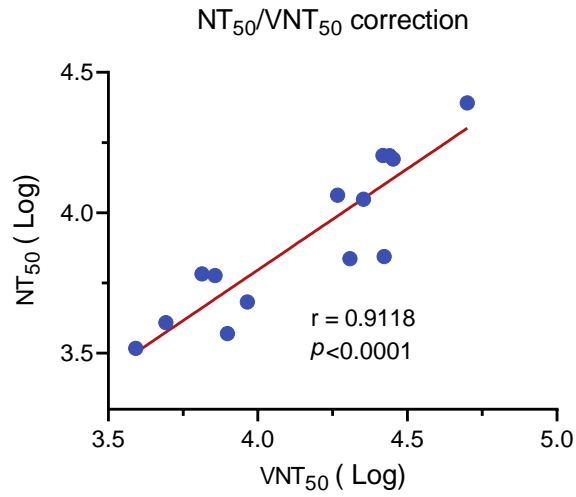
179

180 **Fig. S5.  $S_{Omicron-6P}$  induced high levels of nAbs against pseudovirus of Omicron variant in**  
 181 **hamsters.**

182 **a**  $NT_{50}$  values were determined by VSV-based pseudovirus (Omicron variant) neutralization  
 183 assay (LLOD = 150) ( $n = 12$ ).

184 **b-e** Neutralization curves of 1 (a), 10 (b), 25 (c), and 50 (d) µg  $S_{Omicron-6P}$  induced antibodies  
 185 against pseudotyped and replication-deficient SARS-CoV-2 Omicron at 1 week after second  
 186 vaccination ( $n = 12$ ).

187



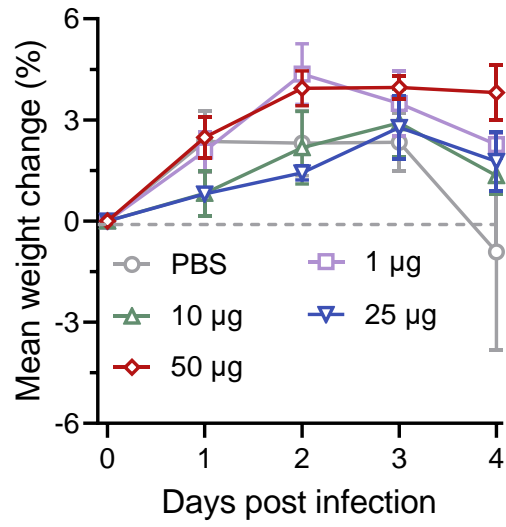
188

189 **Fig. S6. Pearson correlation of VSV-SARS-CoV-2 (Omicron variant) VNT<sub>50</sub> with live**

190 **SARS-CoV-2 (Omicron variant) VNT<sub>50</sub> for  $n = 14$  random selected serum samples from**

191 **hamsters immunized with S<sub>Omicron</sub>-6P.**

192



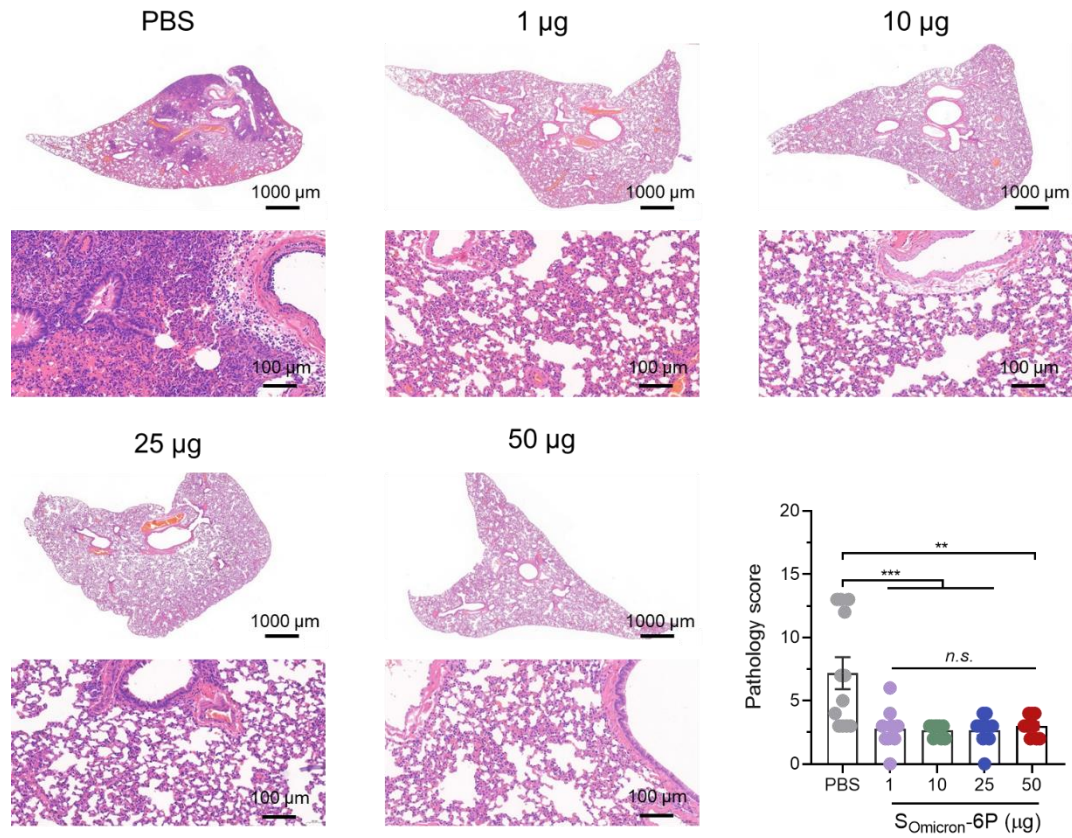
193

194 **Fig. S7. Body weight change in hamsters immunized with PBS or 1, 10, 25, 50 µg S<sub>Omicron-</sub>**

195 **6P from day 0 to day 4 after challenge with Omicron (*n* = 3~4).**

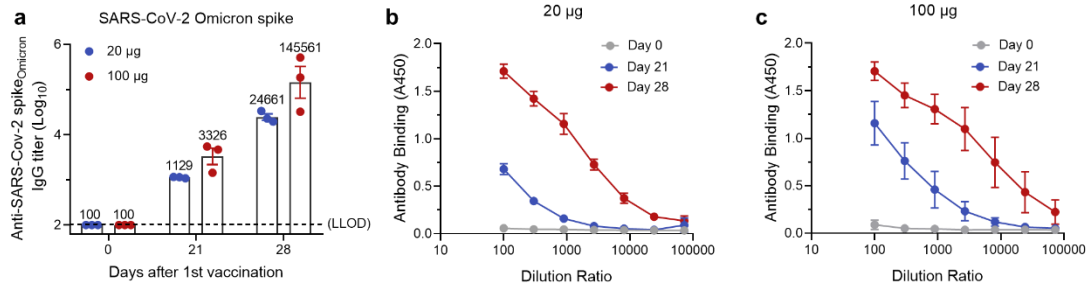
196





197

198 **Fig. S8. Hematoxylin and eosin (H&E) staining of lung sections harvested from PBS or**  
 199 **S<sub>Omicron-6P</sub> (1, 10, 25, 50 µg) vaccinated hamsters after challenge with Omicron at 4 dpi. The**  
 200 **corresponding pathology score of all lung sections from different groups ( $n \geq 9$ ).**  
 201



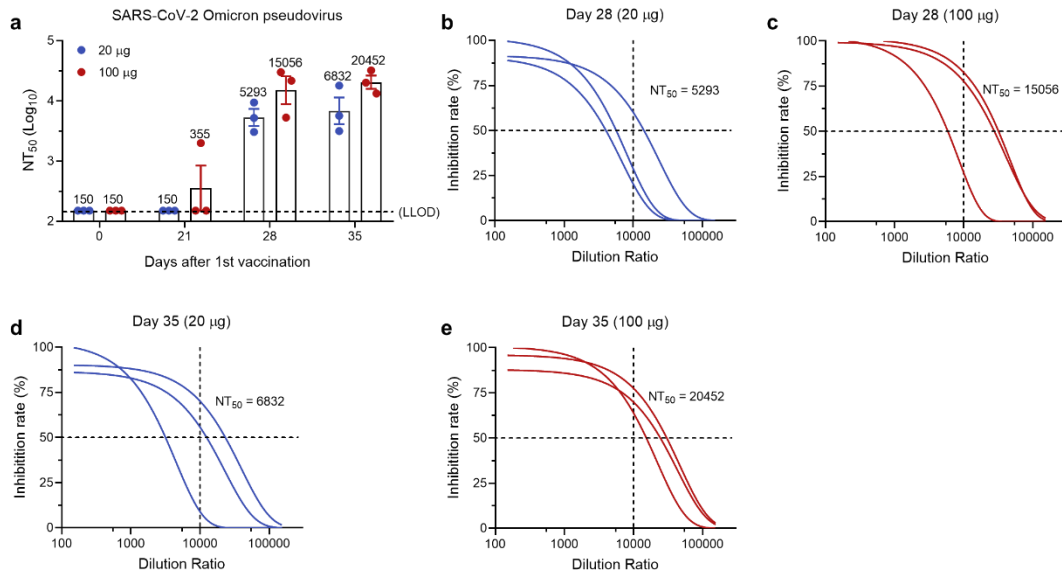
202

203 **Fig. S9. S<sub>Omicron</sub>-6P elicits binding antibodies in macaques.**

204 **a** The Omicron SARS-CoV-2 variant specific IgG antibody titers were determined by ELISA  
 205 (LLOD = 100) ( $n = 3$ ).

206 **b, c** ELISA binding curves of 20 (b) and 100 (c) µg S<sub>Omicron</sub>-6P induced antibodies in macaque  
 207 sera on day 0, 21, 28 after the first immunization ( $n = 3$ ).

208



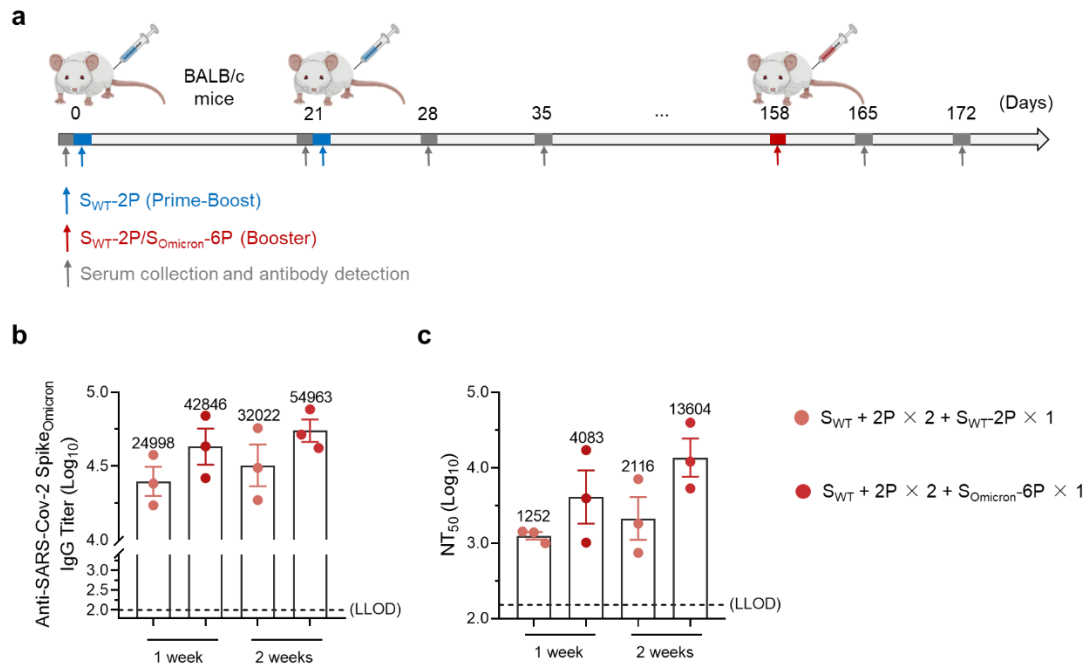
209

210 **Fig. S10. S<sub>Omicron</sub>-6P induced high levels of nAbs against pseudovirus of Omicron variant**  
 211 **in macaques.**

212 **a** NT<sub>50</sub> values were determined by VSV-based pseudovirus (Omicron variant) neutralization  
 213 assay (LLOD = 150) (*n* = 3).

214 **b-e** Neutralization curves of S<sub>Omicron</sub>-6P induced antibodies against pseudotyped and  
 215 replication-deficient SARS-CoV-2 Omicron 1 week (b, c) and 2 weeks (d, e) after the second  
 216 vaccination (*n* = 3).

217



218

219 **Fig. S11 Boosting WT mRNA vaccines with  $S_{Omicron-6P}$  increases protection immune response**  
 220 **against the Omicron variant.**

221 **a.** Schematics showing the immunization and blood sampling schedule of mice immunized with  
 222 heterologous or homologous mRNA vaccines. Female BALB/c mice were first immunized with 10  
 223  $\mu\text{g}$   $S_{WT-2P}$  on day 0 and day 21. On day 158, the mice were immunized with 1  $\mu\text{g}$   $S_{Omicron-6P}$  or  $S_{WT-}$   
 224 2P as a booster shot.

225 **b** The Omicron SARS-CoV-2 variant specific IgG antibody titers were determined by ELISA (LLOD  
 226 = 100) ( $n = 3$ ).

227 **c**  $\text{NT}_{50}$  values were determined by VSV-based pseudovirus (Omicron variant) neutralization assay  
 228 (LLOD = 150) ( $n = 3$ ).

229